

Effect of regional tectonic setting on local fault response to episodes of volcanic activity

Diana C. Roman¹ and Philip Heron²

Received 30 March 2007; revised 6 April 2007; accepted 7 June 2007; published 14 July 2007.

[1] In this study we examine the interaction of tectonic and volcanically-generated stress fields, and their combined effect on patterns of volcanotectonic (VT) seismicity, by calculating Coulomb stress changes on local faults induced by a constant dike inflation event in a background stress field of systematically varying magnitude and orientation. We find that patterns of VT seismicity (earthquake locations and fault-plane solutions) resulting from dike inflation depend strongly on the relative strength and orientation of background tectonic stresses. Patterns of VT seismicity similar to those predicted by our Coulomb stress models have been observed at several recently active volcanoes, and appear to correspond to the relative strength of the regional stress field. Thus, it is critical to consider the regional tectonic setting when interpreting patterns of VT seismicity in terms of magmatic processes. **Citation:** Roman, D. C., and P. Heron (2007), Effect of regional tectonic setting on local fault response to episodes of volcanic activity, *Geophys. Res. Lett.*, *34*, L13310, doi:10.1029/2007GL030222.

1. Introduction

[2] There is substantial evidence for mechanical coupling between crustal faults and magmatic systems. Large earthquakes may release accumulated stress onto a nearby magmatic system, perturbing the system and thus triggering an eruption [e.g., Manga and Brodsky, 2006; Linde and Sacks, 1998]. Conversely, processes leading to physical changes in a magmatic system (e.g., injection or withdrawal of magma) may load stresses onto nearby faults, triggering earthquakes [e.g., Roman, 2005]. Although the triggering mechanisms for these phenomena are not yet fully understood, it is clear that faults in volcanic regions may receive and respond to stresses from both tectonic and magmatic processes. Thus, it is critical to examine how the interaction of tectonically- and magmatically-generated stress fields affects patterns of earthquake activity, in order to accurately interpret earthquake data from volcanic regions and to refine assessments of earthquake and eruption likelihood.

[3] A simple geometric relationship exists between the orientation of a regional (tectonic) stress field, the preferred orientation of a dike with respect to the regional stress field [e.g., Nakamura, 1977], the orientation of a local stress field induced by the inflation of that dike [e.g., Bonafede and Danesi, 1997], and the orientation of fault-plane solutions for earthquakes resulting from stresses induced by dike

inflation [Roman, 2005]. The results of a recent study [Roman, 2005] of Coulomb stress changes induced by the inflation of dike-like magmatic conduits on local faults indicate that a reversal of the sense of slip on suitably-oriented faults should be observable in fault-plane solutions for volcanotectonic (VT) earthquakes [e.g., Lahr et al., 1994] accompanying magma ascent. Specifically, a $\sim 90^\circ$ change in the orientation of the fault-plane solution p-axis relative to the orientation of regional maximum compression (and dike alignment) should be observed even when the amount of dike inflation is relatively small (on the order of one meter). However, a review of well-constrained case studies of stress field response to magmatic activity [Roman and Cashman, 2006] indicates that, while the predicted $\sim 90^\circ$ change in fault-plane solution p-axis orientation is observed in some cases, there are other cases where a change in the sense of fault slip clearly did not occur during the period of volcanic activity. Roman and Cashman [2006] propose several hypotheses to explain differences in patterns of VT seismicity, including differences in magma rheology and differences in regional tectonic setting and associated background crustal stresses. For the latter, it is hypothesized that a strong tectonic stress field might override local stresses induced by magma ascent, such that a change in the sense of slip on local faults does not occur.

[4] In this study, we examine the proposal that differences in regional tectonic setting may explain differences in observed patterns of VT seismicity at active or restless volcanoes. Specifically, we hypothesize that the relative strength of the regional and volcanically-induced stress fields controls the likelihood and sense of slip on faults surrounding the magmatic system. Three possible scenarios are illustrated in Figure 1. In the first scenario (Figure 1a), volcanic stresses dominate over tectonic stresses, and faults slip in a 'reversed' sense (relative to the regional sense of slip). Fault-plane solutions for these slip events have p-axes perpendicular to regional maximum compression (σ_1). In the second scenario (Figure 1b), regional stresses dominate over volcanic stresses, leading to fault slip in the regional sense (fault-plane solution p-axes parallel to regional σ_1). In the third scenario (Figure 1c), regional stresses balance volcanic stresses and faults are effectively 'locked', leading to the appearance of earthquake shadow zones [e.g., Harris, 1998] around the inflating dike. Here, we test this hypothesis by modeling fault slip resulting from dike inflation through calculation of Coulomb stress changes resulting from the interaction of a background (tectonic) stress field and a stress field resulting from dike inflation. Our goal is to assess the extent to which the magnitude and orientation of tectonic stresses affects the pattern of fault slip resulting from stresses produced during magma ascent, to better

¹Department of Geology, University of South Florida, Tampa, Florida, USA.

²School of Earth and Environment, University of Leeds, Leeds, UK.

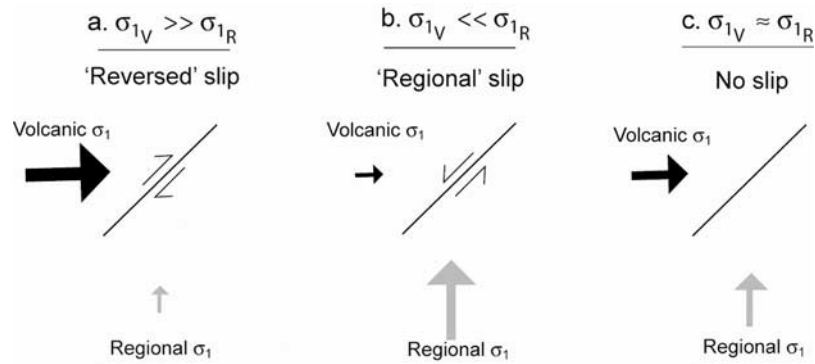


Figure 1. Schematic illustration of three hypothesized relationships between the orientation and magnitude of tectonic stress and volcanically-generated stress, and the likelihood and sense of fault slip. (a) Volcanic stress magnitude greater than tectonic stress magnitude, (b) tectonic stress magnitude greater than volcanic stress magnitude, and (c) approximately equal tectonic and volcanic stress magnitudes. σ_1 refers to the maximum compressive stress axis. ‘Reversed’ slip has fault-plane solution p-axis perpendicular to regional σ_1 and ‘Regional’ slip has fault-plane solution p-axis parallel to regional σ_1 .

explain differences between characteristic patterns of VT seismicity observed during recent eruptions.

2. Methodology

[5] Using Coulomb stress changes as a proxy for expected earthquake locations and fault-plane solutions in the vicinity of an inflating dike [e.g., Roman, 2005], we model fault response to dike inflation in a range of simulated compressional and strike-slip tectonic regimes. We use the boundary-element code package Coulomb 2.6 [Toda *et al.*, 1998], which allows calculation of changes in Coulomb stress caused by an inflating rectangular source on faults of specified location, orientation, and sense of slip in a prescribed regional stress field. Increases in Coulomb stress (effectively, increases in the amount of shear stress relative to normal stress) on an existing fault correspond to an increase in the probability of failure on that fault [King *et al.*, 1994]. All calculations are made in a homogeneous half-space with elastic moduli appropriate for the shallow crust (shear modulus of 3.2×10^4 MPa, Poisson’s ratio of 0.25, and an effective coefficient of internal friction of 0.4). In this study, dike inflation is always in the direction of regional σ_3 , and is instantaneous. This study also assumes that pore pressure is constant in all cases, although in real systems changes in pore fluid pressure may significantly affect fault response by allowing slip on fault planes poorly oriented with respect to maximum compression (σ_1) [e.g., Cocco and Rice, 2002]. Due to model limitations, we only explore the effects of absolute compression (neglecting extensional tectonic regimes) in the present study.

[6] The study involved a set of numerical experiments in which a specified dike inflation event (1 m inflation of a 1-km-long vertical dike) occurred in a background stress field of systematically varying magnitude and orientation. We model differential, as opposed to absolute, background stress magnitude, where a background stress field is defined as ‘isotropic’ when the magnitudes of the three principal regional stress axes are equal (i.e., $\sigma_1 = \sigma_2 = \sigma_3 = 0$), and ‘deviatoric’ when there is some difference between them. Except where specified, we allowed the model code to set faults to an optimal orientation and rake, where an optimally-oriented fault is positioned to receive the greatest

(positive) Coulomb stress change in the modeled scenario. Thus the models presented here are ‘best-case scenarios’ for situations in which the true fault orientation is generally undeterminable. In this paper we present examples involving optimally-oriented strike-slip faults, which best illustrate the primary results of our full set of experiments.

3. Effect of Tectonic Stresses on Fault Slip Induced by Dike Inflation

[7] Patterns of fault slip (i.e., earthquake location and fault-plane solution) in response to dike inflation depend strongly on the relative strength and orientation of tectonic stresses (Figure 2). In an isotropic tectonic stress field (this is an unrealistic scenario but it represents an endmember to the spectrum of expected earthquake patterns), stresses induced by dike inflation dominate local fault behavior (Figure 2a). Strike-slip faulting with a ‘reversed’ sense of slip (fault-plane solution p-axis orientation $\sim 90^\circ$ to regional σ_1) is expected in a large region extending laterally from the walls of the inflating dike, and fault-plane solution orientations for inflation-induced earthquakes will be heterogeneous and dependent on the location of the fault relative to the inflating dike. No earthquake shadow zones appear in this scenario. As the difference between the magnitude of the two horizontal regional stress axes (or axes perpendicular to the direction of dike propagation) increases (the weakly deviatoric scenario), the area in which faulting with a reversed sense of slip is predicted becomes smaller, and fault-plane solution orientations remain heterogeneous but are dominantly ‘ $\sim 90^\circ$ rotated’ (p-axes perpendicular to regional σ_1) and ‘regional’ (p-axes parallel to regional σ_1) (Figure 2b). In this scenario, shadow zones are present at some distance from the inflating dike. As the difference between the magnitude of the two horizontal regional stress axes becomes large (the strongly deviatoric scenario), all faults in the walls of the dike lock and no fault slip is expected in this region (Figure 2c). However, faulting with a regional sense of slip (fault plane solution p-axes parallel to regional σ_1) is predicted in zones extending from the tips of the inflating dike, which form a characteristic ‘dogbone’ pattern [e.g., Hill, 1977] as illustrated by the heavy black lines in Figure 2c. Earthquakes induced by dike inflation in a

strongly deviatoric regional stress field are expected to have fault-plane solutions that are homogeneous in orientation.

[8] The threshold values of relative regional stress magnitude at which the behavior of faults in the vicinity of the

inflating dike changes depend on a combination of a) the amount of instantaneous dike opening (as opposed to total dike width), and b) the length of the dike. In general, the threshold values increase with increasing amounts of dike inflation and decrease with increasing dike length. Thus, depending on dike geometry and degree of inflation, observed fault response may vary from eruption to eruption at a given volcano.

4. Discussion and Conclusions

[9] Modeled patterns of VT earthquakes resulting from stresses produced during dike inflation in the presence of tectonic stress fields with relative magnitudes typical for the Earth's crust [e.g., McGarr and Gay, 1978, Feuillet *et al.*, 2004] are in general agreement with patterns of VT seismicity observed prior to and during episodes of volcanic activity. Roman and Cashman [2006] describe two characteristic patterns of VT seismicity apparent in a review of published VT data sets. We illustrate these two patterns in Figure 3 with seismic data from two recent eruptions in Japan [e.g., Fukuyama *et al.*, 2001]: The 2000 eruption of Mt. Usu and the 2000 eruption and dike intrusion at Miyake-jima Volcano (earthquake locations and fault-planes solutions provided by the Japan NIED F-NET and Japan Meteorological Agency). The first pattern involves VT earthquakes with hypocenters randomly distributed within a cluster proximal to the eruptive vent, with fault-plane solution p-axes oriented both approximately perpendicular and parallel to regional σ_1 (e.g., Figure 3a); the second pattern involves VT earthquakes with propagating hypocenters and fault-plane solution p-axes parallel to regional σ_1 (e.g., Figure 3b). The VT earthquakes recorded at Miyake-jima Volcano during the 2000 episode form one of the best examples of a dogbone epicenter distribution observed to date [Toda *et al.*, 2002] (Figure 3b).

[10] The patterns of VT seismicity illustrated in Figure 3 are in strong general agreement with the patterns of faulting predicted in our models of fault response to dike inflation in weakly and strongly deviatoric tectonic stress fields (Figures 2b and 2c). The volcanoes of Japan occupy a wide range of tectonic settings, from extensional on the southern island of Kyushu to compressional on the islands of Shikoku, Honshu, and Hokkaido [e.g., Kato *et al.*, 1998]. Strain rate data [e.g., Sagiya *et al.*, 2000] from the dense continuous GPS network (GEONET) run by the Geographic

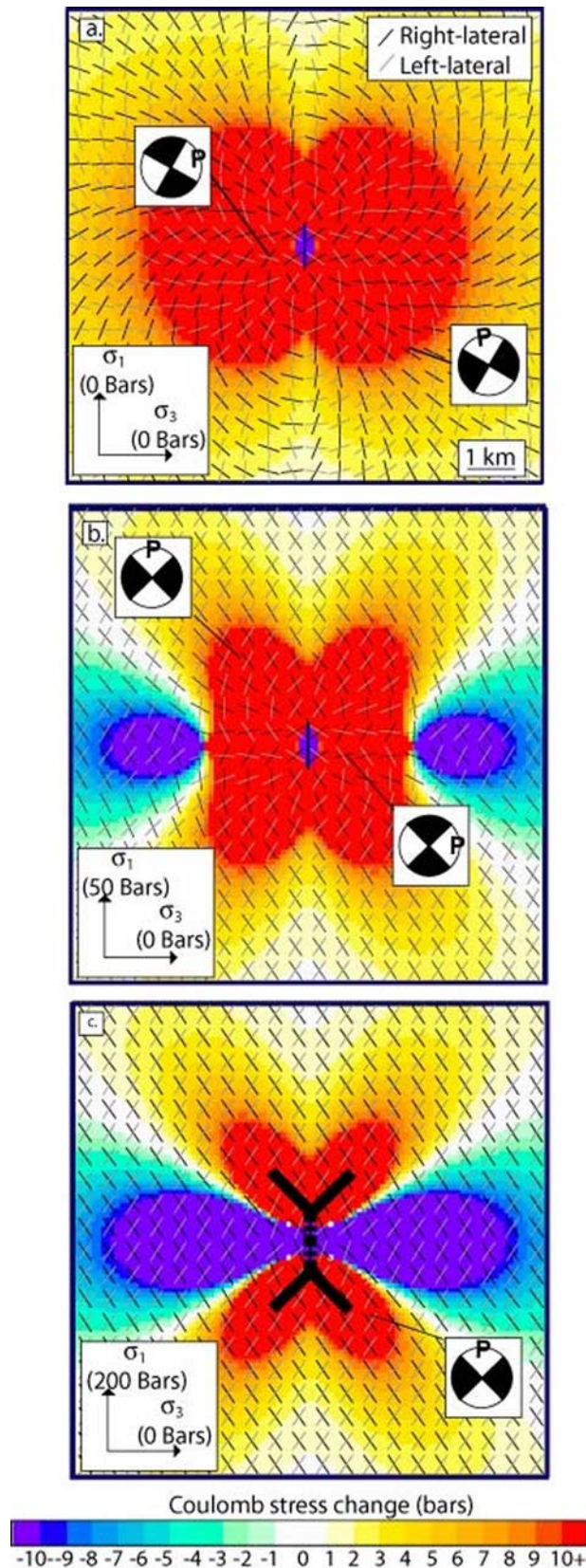


Figure 2. Coulomb stress models of fault response to dike inflation in a tectonic stress field of variable relative magnitude. (a) Fault response to dike inflation in an isotropic tectonic stress field. (b) Fault response to dike inflation in a 'weakly deviatoric' tectonic stress field. (c) Fault response to dike inflation in a 'strongly deviatoric' tectonic stress field (dogbone limbs shown by heavy black lines, model dike shown by dot-dash line). In all cases the inflating dike is vertically oriented, 1 km long, and inflates by 1 m. Colors correspond to the approximate magnitude of Coulomb stress change on modeled faults. Thin black (right-lateral) and gray (left-lateral) lines show the optimal fault orientation (in the combined stress field) at every point around the dike. Representative fault-plane solutions are also shown. Insets show the relative magnitude of modeled tectonic stress.

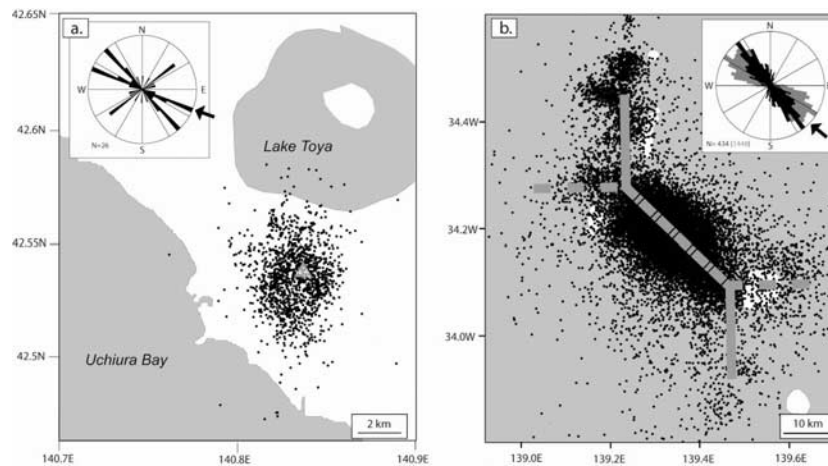


Figure 3. (a) Location of earthquakes (black dots) recorded during the 2000 eruption of Mt. Usu, Japan between March 27–April 1, 2000 (data from the Japan Meteorological Agency). Inset shows a rose diagram of fault-plane solution p-axis azimuths for the same period (data from the Japan National Research Institute for Earth Science and Disaster Prevention (NIED) F-net). (b) Location of earthquakes recorded during the 2000 eruption and dike intrusion at Miyake-jima, Japan between June 1–Dec 31, 2000 (data from NIED F-net). The dogbone pattern formed by the earthquake epicenters is indicated by heavy gray lines (dashed where dogbone limbs are not represented by earthquakes, dot-dashed in region of dike emplacement where earthquakes may represent tensile failure at a propagating dike tip). Inset shows a rose diagram of fault-plane solution p-axis azimuths for the same period (gray for entire data set, black for earthquakes comprising dogbone limbs (marked with solid gray lines on map) - data from NIED F-net). N gives number of fault-plane solutions. Heavy arrows on inset rose diagrams show approximate orientation of regional maximum compressive stress.

Survey Institute (GSI) in Japan indicate the existence of exceptionally high crustal strain rates (which may be taken as a proxy for differential stress magnitudes) in the region directly offshore of the Izu Peninsula, where a dogbone distribution of earthquakes with ‘regional’ fault-plane solutions was observed during the 2000 volcanic activity at Miyake-jima Volcano (Figure 3b) [Toda *et al.*, 2002; Fukuyama *et al.*, 2001]. The data from GEONET also indicate the existence of lower strain rates on south-central Honshu, where a random distribution of VT hypocenters and a $\sim 90^\circ$ perturbation in fault-plane solution orientation was observed during the 2000 eruption of Mt. Usu (Figure 3a) [Fukuyama *et al.*, 2001; Ueno *et al.*, 2002]. Thus, it appears that the differences in patterns of VT seismicity observed at these two volcanoes may be related to differences in the relative magnitude of tectonic stresses across the Japanese island arc. However, it is important to note that other factors may have contributed to the difference in VT seismicity activity observed at these two volcanoes. Roman and Cashman [2006] propose that the viscosity and/or rheology of an ascending magma may influence patterns of VT seismicity, and note significantly different magma compositions and crystal contents erupted at Mt. Usu and Miyake-jima Volcano in 2000 [Nogami and Hirabayashi, 2002; Amma-Miyasaka *et al.*, 2005]. We further note that a significant percentage of the VT earthquakes occurring during the 2000 Miyake-jima event were not located in the modeled dogbone limbs (represented by solid heavy lines in Figures 2c and 3b) but in an elongated zone corresponding to the location of our model dike (dot-dashed heavy line in Figure 2c) and to the location of the inflating dike extending from Miyake-jima as modeled from surface deformation data [Nishimura *et al.*, 2001] (dot-dash line in Figure 3b). As these hypocenters propagated with

time [Toda *et al.*, 2002], it is likely that they represent formation of the dike itself (tensile failure at the propagating dike tip) as opposed to fault slip in the solid rock surrounding the dike, and thus a separate VT source process from the one we have examined in this study.

[11] Faults with an optimal orientation (as modeled here) may or may not exist around a given dike, and the orientation and location of pre-existing faults will strongly influence the spatial pattern, fault-plane solutions, and degree of fault-plane solution heterogeneity of VT earthquakes. For example, fault-plane solutions for Miyake-jima do not show model-predicted homogeneity in orientation (compare Figure 2c and Figure 3b inset). This may reflect heterogeneous fault orientations in the vicinity of the Miyake-jima dike, although the (likely) possibility that the spread in p-axis orientations shown in Figure 3b reflects errors in the fault-plane solution data cannot be discounted. Non-optimally-oriented faults with a wide range of orientations may also slip in response to dike inflation [Roman, 2005], so we believe that the general characteristics of VT seismicity in most cases will be similar to our model results.

[12] There are several other real effects that have not been accounted for in our models. First, we model instantaneous dike inflations and do not account for gradual dike opening that would produce lower stress rates that could result in different patterns of seismicity [Toda *et al.*, 2002]. Because of this we have modeled relatively small amounts of instantaneous dike inflation (one meter) that are more likely to be representative of true rates of dike inflation. We have also neglected dike propagation, focusing only on the inflation of an emplaced dike and the effect on pre-existing faults. Finally, we have not considered earthquake magnitude. Coulomb stress change modeling makes no explicit or implicit prediction of earthquake magnitude, only of earth-

quake probability. Thus, the important question of whether and under what circumstances magma ascent and dike inflation may trigger large earthquakes during episodes of volcanic unrest remains unresolved.

[13] In conclusion, we find that patterns of VT seismicity are controlled by the differential magnitude of principal regional stresses in compressional and strike-slip tectonic regimes. Furthermore, we find that models of VT seismicity resulting from dike inflation that incorporate background tectonic stresses may be used to explain differences in patterns of VT seismicity at two recently active volcanoes in Japan located in tectonic settings characterized by different relative stress magnitudes. Thus, interpretations of VT seismicity should always account for the possible effects of tectonic stresses. Ultimately, the interactions between tectonic stresses, other local stresses, and stresses resulting from magma ascent are complex and can vary from eruption to eruption, even at a single volcano. However, careful consideration of the relative importance of these controlling factors will lead to improved interpretations of VT earthquake activity and refined forecasts of volcanic activity based on precursory seismicity.

[14] **Acknowledgments.** Thank you to Shinji Toda for advice and assistance with Coulomb 2.6 and to the Japan National Research Institute for Earth Science and Disaster Prevention (NIED) for assistance with data retrieval from F-Net. We also thank Hitoshi Yamasato of the Japan Meteorological Agency for providing the earthquake locations from Mt. Usu, and Valerio Acocella and an anonymous reviewer for their thoughtful reviews. DCR acknowledges support from the Natural Environment Research Council (UK) and PH acknowledges support from the Nuffield Foundation (UK).

References

- Amma-Miyasaka, M., M. Nakagawa, and S. Nakada (2005), Magma plumbing system of the 2000 eruption of Miyakejima Volcano, Japan, *Bull. Volcanol.*, *67*, 254–267.
- Bonafede, M., and S. Danesi (1997), Near-field modifications of stress induced by dyke injection at shallow depth, *Geophys. J. Int.*, *130*, 435–448.
- Cocco, M., and J. R. Rice (2002), Pore pressure and poroelasticity effects in Coulomb stress analysis of earthquake interactions, *J. Geophys. Res.*, *107*(B2), 2030, doi:10.1029/2000JB000138.
- Feuillet, N., C. Nostro, C. Chiarabba, and M. Cocco (2004), Coupling between earthquake swarms and volcanic unrest at the Alban Hills Volcano (central Italy) modeled through elastic stress transfer, *J. Geophys. Res.*, *109*, B02308, doi:10.1029/2003JB002419.
- Fukuyama, E., A. Kubo, H. Kawai, and K. Nonomura (2001), Seismic remote monitoring of stress field, *Earth Planets Space*, *53*, 1021–1026.
- Harris, R. A. (1998), Introduction to special section: Stress triggers, stress shadows, and implications for seismic hazard, *J. Geophys. Res.*, *103*, 24,347–24,358.
- Hill, D. P. (1977), A model for earthquake swarms, *J. Geophys. Res.*, *82*, 1347–1352.
- Kato, T., G. S. El-Fiky, and E. N. Oware (1998), Crustal strains in the Japanese islands as deduced from dense GPS array, *Geophys. Res. Lett.*, *25*, 3445–3448.
- King, G. C. P., R. S. Stein, and J. Lin (1994), Static stress changes and the triggering of earthquakes, *Bull. Seismol. Soc. Am.*, *84*, 935–953.
- Lahr, J. C., B. C. Chouet, C. D. Stephens, J. A. Power, and R. A. Page (1994), Earthquake classification, location, and error analysis in a volcanic environment: Implications for the magmatic system of the 1989–1990 eruptions at Redoubt volcano, Alaska, *J. Volcanol. Geotherm. Res.*, *62*, 137–152.
- Linde, A. T., and I. S. Sacks (1998), Triggering of volcanic eruptions, *Nature*, *395*, 888–890.
- Manga, M., and E. E. Brodsky (2006), Seismic triggering of eruptions in the far field: Volcanoes and geysers, *Annu. Rev. Earth Planet. Sci.*, *34*, 263–291.
- McGarr, A., and N. C. Gay (1978), State of stress in the Earth's crust, *Annu. Rev. Earth Planet. Sci.*, *6*, 405–436.
- Nakamura, K. (1977), Volcanoes as possible indicators of tectonic stress orientation: Principle and proposal, *J. Volcanol. Geotherm. Res.*, *2*, 1–16.
- Nishimura, T., S. Ozawa, M. Murakami, T. Sagiya, T. Tada, M. Kaidzu, and M. Ukawa (2001), Crustal deformation caused by magma migration in the northern Izu islands, Japan, *Geophys. Res. Lett.*, *28*, 3745–3748.
- Nogami, K., and J. Hirabayashi (2002), Nature and origin of volcanic ash in the 2000 eruption of Usu Volcano, southwestern Hokkaido, Japan, *Earth Planets Space*, *54*, 993–998.
- Roman, D. C. (2005), Numerical models of volcanotectonic earthquake triggering on non-ideally oriented faults, *Geophys. Res. Lett.*, *32*, L02304, doi:10.1029/2004GL021549.
- Roman, D. C., and K. V. Cashman (2006), The origin of volcanotectonic earthquake swarms, *Geology*, *34*, 457–460.
- Sagiya, T., S. Miyazaki, and T. Tada (2000), Continuous GPS array and present-day crustal deformation of Japan, *Pure Appl. Geophys.*, *157*, 2303–2322.
- Toda, S., R. S. Stein, P. A. Reasenberg, and J. H. Dieterich (1998), Stress transferred by the $M_w = 6.9$ Kobe, Japan, shock: Effect on aftershocks and future earthquake probabilities, *J. Geophys. Res.*, *103*, 24,543–24,565.
- Toda, S., R. S. Stein, and T. Sagiya (2002), Evidence from the AD 2000 Izu islands earthquake swarm that stressing rate governs seismicity, *Nature*, *419*, 58–61.
- Ueno, H., H. Mori, Y. Usui, and J. Miyamura (2002), Earthquake swarm immediately before and after the beginning of the 2000 eruption of the Usu volcano monitored by the regional seismic network, *Bull. Volcanol. Soc. Jpn.*, *47*, 689–694.

P. Heron, School of Earth and Environment, University of Leeds, Leeds LS2 9JT, UK.

D. C. Roman, Department of Geology, University of South Florida, Tampa, FL 33620, USA. (droman@cas.usf.edu)